RSC Advances

ROYAL SOCIETY OF CHEMISTRY

www.rsc.org/advances

Structure and electrical properties of lead-free $Sr_{1-x}(K,Ce)_{x/2}(Na_{0.5}Bi_{0.5})Bi_4Ti_5O_{18}$ piezoelectric ceramics

Zhongran Yao[1], Ruiqing Chu[1 *], Zhijun Xu[1], Jigong Hao[1], Juan Du[1], Guorong Li[2]

1. College of Materials Science and Engineering, Liaocheng University, Liaocheng 252059, People's Republic of China;
2. The State Key Lab of High Performance Ceramics and Superfinemicrostructure, Shanghai Institute of Ceramics, Chinese Academy of Science, Shanghai 200050, People's Republic of China.

Abstract: Bismuth layer-structured ferroelectrics, $Sr_{1-x}(K,Ce)_{x/2}(Na_{0.5}Bi_{0.5})Bi_4Ti_5O_{18}$ (KCSNBT-x, x=0.0, 0.1, 0.2 and 0.3), were prepared by a conventional solid-state reaction method. The X-ray diffraction analysis suggested that the substitution formed layered perovskite structure. Plate-like morphologies for the grains were clearly observed for all samples. The activation energy value of the ionic conductivity suggested defects were related to oxygen vacancies. Excellent electrical properties (e.g., d_{33}~21pC/N, $2P_r$~16.4μC/cm^2 and T_c~567□) are simultaneously obtained in the ceramic with x=0.3. Additionally, thermal annealing studies indicated that piezoelectric constant (d_{33}) of KCSNBT-0.1 ceramic remains almost unchanged (22 pC/N, only decrease by 4 %) at temperatures below 400℃, demonstrating the ceramic is the promising candidates for high-temperature applications.

Keywords: Bismuth layer-structured; solid-state reaction; X-ray diffraction; electrical properties

1. Introduction

Bismuth layer-structured ferroelectrics (BLSFs), known as Aurivillius family of oxides, have been considered as one kind of promising lead-free piezoelectrics in

* Corresponding author. Tel. / fax: +86 635 8239106. E-mail address: ruiqingchu@sohu.com or rqchu@lcu.edu.cn .

high-temperature applications [1, 2]. Compared with traditional perovskite structure, the structure of these ferroelectrics, represented as $(Bi_2O_2)^{2+}(A_{m-1}B_mO_{3m+1})^{2-}$, consists of $[Bi_2O_2]^{2+}$ layers interleaved with perovskite block of $[A_{m-1}B_mO_{3m+1}]^{2-}$ units along the *c*-axes, where the *A*-site in the perovskite block can be occupied by 12-coordinated cations such as Bi^{3+}, La^{3+}, Ba^{2+}, Sr^{2+},Ca^{2+}, etc, while the *B*-site can be occupied by 6-coordinated cations such as Ti^{4+}, Nb^{5+}, Ta^{5+}, W^{6+}, Mo^{6+}, Co^{3+}, etc. In addition, the *m*, in the range of 1-5, represents the number of perovskite blocks, and the ferroelectric and dielectric properties of BLSFs are strongly dependent on the value of it [3-7]. The BLSFs ceramics possess some outstanding electrical properties, such as high Curie temperature, low dielectric loss, excellent fatigue endurance and low aging rate, making BLSFs a promising candidate for ferroelectric non-volatile random access memory (FRAM) storage devices [8].

$SrNa_{0.5}Bi_{4.5}Ti_5O_{18}$ (abbreviated as SBT), as the *m*=5 member of the Aurivillius family where Bi_2O_2 layers alternate with ($SrNa_{0.5}Bi_{2.5}Ti_5O_{16}$) perovskite blocks built by five TiO_6 octahedral layers and hosting Sr and Bi at the *A* site, has drawn a special attention because of its high Curie temperature[9]. However, as other BLSF compounds, this material exhibits relatively low piezoelectric coefficients (d_{33}) and low remanent polarization ($2P_r$) because of the spontaneous polarization is restricted in *a*-*b* plane[9, 10]. To overcome this shortcoming, many efforts have been paid to improve its dielectric and piezoelectric properties by adding some additives in *A*-site and/or *B*-site [11, 12]. In those studies, *A*-site substitution is more effective than that of *B*-site substitution because that the cations in *B*-site have the similar size and hardly make a major contribution to the polarization process for BLSFs. For instance, Ji et al[13] reported that the $SrNa_{0.5}Bi_{4.5}Ti_5O_{18}$+1wt%$CeO_2$ sample shows excellent Curie temperature (586□) and very large piezoelectric coefficient (24pC/N). Chen et al[10]. have

investigated the properties of $Sr_{2-x}(Na, K)_xBi_4Ti_5O_{18}$ composite ceramics and found that the piezoelectric constant d_{33} and remnant polarization $2P_r$ were improved to be 20 pC/N and 20μC/cm^2, respectively, whereas the Curie temperature is only 324℃. Additionally, it was found that (MCe) (M = Li, Na, K) dopants can efficiently enhance the piezoelectric coefficients for even-layer structured Aurivillius type compounds compared to the pure composition [14, 15].

Nevertheless, very little is known about the detailed electrical properties on (KCe) modified $Sr(Na_{0.5}Bi_{0.5})Bi_4Ti_5O_{18}$ (SNBT) ferroelectric ceramics. Therefore, in the present work, *A*-site (KCe)-doped $Sr(Na_{0.5}Bi_{0.5})Bi_4Ti_5O_{18}$ ceramics were prepared by conventional solid state sintering method, and the effect of (KCe) modification for A-site on their electrical properties was investigated. Additionally, the underlying physical mechanisms for enhanced piezoelectricity and electrical conductivity have been addressed.

2. Experimental details

$Sr_{1-x}(K,Ce)_{x/2}(Na_{0.5}Bi_{0.5})Bi_4Ti_5O_{18}$ (abbreviated as KCSNBT-*x*, *x*=0, 0.1, 0.2 and 0.3) ceramics were prepared by conventional solid-state reaction method using reagent-grade metal oxides or carbonate powders of K_2CO_3(99%, Sinopharm Chemical Reagent Co., Ltd., China), CeO_2(99.95%, Sinopharm Chemical Reagent Co., Ltd., China), Bi_2O_3 (99.99%, Sinopharm Chemical Reagent Co., Ltd., China), $SrCO_3$ (99%, Sinopharm Chemical Reagent Co., Ltd., China), TiO_2 (99.5%, Sinopharm Chemical Reagent Co., Ltd., China) and Na_2CO_3 (99.49%, Sinopharm Chemical Reagent Co., Ltd., China) as the starting materials. All raw materials were weighed at stoichiometric proportion and then mixed by planetary ball milling in a polyethylene with stabilized zirconia balls for 15 h, using ethanol as the solvent. After drying, the mixed powders were calcined at 800°C for 2 h. After calcination, the

mixture was milled again for 12 h, and then dried. The powders were mixed with an appropriate amount of polyvinyl butyral (PVB) binder, and pressed into pallets with a diameter of 12 mm and a thickness of 0.7 mm under the pressure of about 200MPa. After burning off PVB at 850□, the ceramics were sintered in an alumina crucible at 1180℃for 3 h. For the electric measurements, disk samples with about 0.3 mm in thickness were used.

The density of the sintered ceramics was measured by means of the Archimedes method. The crystal structure of the ceramics was determined by X-ray diffraction (XRD) using a Cu Kα radiation (λ=1.54178 Å) (D8 Advance, Bruker Inc., Germany). The surface morphology of the ceramics was observed by scanning electron microscope (SEM) (JSM-6380, Japan). The ferroelectric hysteresis loops were measured through standardized ferroelectric test system (TF2000, Germany). The temperature dependence of dielectric properties and impedance spectroscopy for the samples was performed using a Broadband Dielectric Spectrometer (Novocontrol Germany). The samples were polarized in silicon oil in the range of 150-180℃ for 20 min, and piezoelectric measurements were carried out with a quasi-static d_{33}-meterYE2730 (SINOCERA, China).

3. Results and discussion

The X-ray diffraction spectra of KCSNBT-x ceramics (x=0.0, 0.1, 0.2, 0.3) in the 2θ range of (a) 20-50° and (b) 28-32° was plotted in **Fig.1**. As shown in **Fig.1(a)**, the Aurivillius structure can be identified by indexing all the diffraction peaks on the basis of an orthorhombic cell (PDF#No.05-0626)[13], indicating that the K^+ and Ce^{3+} ions diffused into the A-site lattice and formed solid solutions as expected. Meanwhile, it is obvious that the highest diffraction peak of KCSNBT-x ceramics is (10$\underline{11}$) orientation, which is consistent with the fact that the strongest diffraction peak in

BLSFs [16]. In addition to the main Aurivillius phase, secondary phase: $Bi_2Ti_2O_7$ (PDF#No. 32-0118, labeled by *) in the KCSNBT-*x* samples can also be detected regardless the existence of (KCe), as shown in **Fig.1(b)**. It seems that this peak could be related to the volatilization of bismuth species at elevated temperatures[17]. Similar deficiency behavior of bismuth species was also found during the sintering of another bismuth-layered compound-$SrBi_4Ti_4O_{15}$[18, 19]. In order to further confirm the crystallographic evolution of KCSNBT-*x* ceramics, the lattice parameters of the samples were calculated and shown in the inset part of **Fig. 1(a)**. It is found that the lattice parameters *a*, *b*, and *c* varied with increasing *x* values, demonstrating that the (KCe) substitution reduced the lattice distortion of SNBT-based ceramics. Such a lattice distortion can be attributed to the replacement of the *A*-site Sr^{2+} by K^+ and Ce^{3+}, and it is supposed to lead to enhanced electrical properties.

The SEM images of the surface morphologies of KCSNBT-*x* ceramics (*x*=0.0, 0.1, 0.2, 0.3) were displayed in **Fig.2**. It is found that the grains of all the samples are all well-packed and the pore-free microstructures were presented. In addition, (KCe)-substituted SNBT ceramics have uniform grain size, indicating that the increasing doping with (KCe) does not change the microstructure dramatically. Due to the structurally highly anisotropic grain growth rate in the direction of the *a*-*b* plane and the lower surface energies of the (001) planes induced predominantly during sintering, all the specimens are composed of plate-like grains, which is a typical characteristic of Aurivillius ceramics[13]. Moreover, all ceramics have a high relative density ρ_{rd} (>96%), suggesting all samples have been well sintered.

Temperature dependence of dielectric constant (ε) and loss ($\tan\delta$) of KCSNBT-*x* ceramics (*x*=0.0, 0.1, 0.2, 0.3) measured at 10kHz is depicted in **Fig.3**. Two phase transitions were observed at ~400 ℃ and ~550 ℃, corresponding to the phase

transitions of ferroelectric-ferroelectric transition and ferroelectric-paraelectric[20]. Such phenomenon was also reported in Ca-doped $SrNa_{0.5}Bi_{4.5}Ti_5O_{18}$ ceramics[13]. In addition, **Fig.3** clearly shows that the value of Curie temperature (T_c) corresponding to the ferro-paraelectric phase transition of ferroelectrics is slightly increased from 562℃ to 570℃, which is higher than the reported results in other Aurivillius material systems (**Table 1**). Moreover, as shown **Fig. 3**, the dielectric loss values were found to be very low (less than 7%) and very stable when the measurement temperature is below 400℃ for all compositions. These results exhibit that the KCSNBT-*x* ceramics possessed the high stability of dielectric behavior, which is of great importance for high-temperature devices applications. When the temperature is above 500℃, the tanδ value significantly increased arising from the space charge carriers induced by the increase of electrical conductivity[21].

Table 1

Comparison of polarization ($2P_r$), Curie temperature (T_c) and piezoelectric constant (d_{33}) of KCSNBT-*x* ceramics with other Aurivillius material systems.

Materials	$2P_r$ ($\mu C \cdot cm^{-2}$)	T_c (℃)	d_{33} ($pC \cdot N^{-1}$)	Reference
KCSNBT-*x*	16.4	567	21	Current work
SBTi-$(Na,K)_x$	20	324	20	10
C_xSBN	15	552	18	16
SBBT	1.4	535	12	22
SNBT	-	535	17	23
SBN	-	440	20	24

It is well known the nature of the phase transition is determined by calculating the degree of diffusion (γ) in the measured dielectric constant by modifying Curie-Weiss law[5]:

$$\frac{1}{\varepsilon}-\frac{1}{\varepsilon_{\mathrm{m}}}=\frac{(T-T_{\mathrm{m}})^{\gamma}}{C}(1\le\gamma\le 2,\ T>T_{\mathrm{m}}) \quad (1)$$

Where, ε is the dielectric constant, ε_{m} is the dielectric constant maximum, T is the temperature ($>T_{\mathrm{c}}$), T_{m} is the temperature at the dielectric peak, γ is the relaxation strength and C is the Curie constant, respectively. The value of γ is from 1 (normal ferroelectrics) to 2 (complete diffuse phase transition). The inset of **Fig.3** shows the plots of $\ln(1/\varepsilon-1/\varepsilon_{\mathrm{m}})$ *versus* $\ln(T-T_{\mathrm{m}})$ at 10 kHz for SNBT, KCSNBT-0.1, KCSNBT-0.2, and KCSNBT-0.3 ceramics. It is observed that the values of degree of diffusion (γ) for all ceramics can be described by two different temperature regions with inflexion at $\ln(T-T_{\mathrm{m}})\sim3.0$, under which the degree of diffusion (γ) is obtained (γ=1.82-1.87), while above which the values of degree of diffusion are much lower (γ=1.23-1.41). This phenomenon could be related to the structural distortion originated from the increasing oxygen vacancies for SNBT ceramic at high temperature[25]. Additionally, the values of γ for all samples are found to be increased with increasing (KCe) concentration and all the values are close to the degree of diffusion (γ) reported for BLSFs ceramics, indicating that the addition of (KCe) in the SNBT ceramic intensifies the diffusive-type phase transition[22]. This can be attributed to the grain size dependence of relaxor behaviour in micro compositional fluctuations[5]. Such a transition from relaxor-like behavior to relaxor-ferroelectric behavior has been observed in other BLSFs [26].

Table 2

Room temperature electrical properties of KCSNBT-*x* ceramics.

Samples (x)	ε	tanδ (%)	T_c (℃)	E_a (eV)	ρ_{rd} (%)	E_c (kV/cm)	$2P_r$ ($\mu C \cdot cm^{-2}$)	d_{33} ($pC \cdot N^{-1}$)
0.0	267	3.4	562	0.80	96.7	34	8	20
0.1	291	1.2	563	0.78	96.9	36	11	23
0.2	293	1.4	564	0.66	97.3	50	12.8	21
0.3	291	3.0	567	0.54	97.4	59	16.4	21

Fig.4 shows the DC resistivity of KCSNBT-x ceramics as a function of reciprocal temperature. The resistivity of all compositions is higher than 10^5 Ω·cm at 525℃. This is important for high temperature piezoelectric sensor applications. Furthermore, the behavior of temperature dependent resistivity follows the Arrhenius relationship:

$$\rho = A\exp(-E_a/k_B T) \quad (2)$$

where A is a pre-exponential factor constant, E_a is the activation energy of the mobile charge carriers, k_B is the Boltzmann constant and T is the absolute temperature[16]. The activation energy is shown in the inset of **Fig. 4** and **Table 2**. It is found that the values of activation energy E_a of KCSNBT-x ceramics, calculated by linear fitting of the data points, were calculated to be 0.8 eV, 0.78 eV, 0.66 eV and 0.54 eV for SNBT, KCSNBT-0.1, KCSNBT-0.2 and KCSNBT-0.3 ceramics, respectively. The results were close to the activation energy values of the ionic conductivity by oxygen vacancies in perovskite type ferroelectric oxides[27-29].

Fig.5 (a) shows P-E hysteresis of KCSNBT-x ceramics measured at 10Hz frequency under a maximum electric field 140kV/cm and at temperature 180℃. The measured remnant polarization ($2P_r$) and coercive field (E_c) values with varying (KCe) content (x) in SNBT ceramics are listed in **Table 2**. It is evident that the remanent

polarization ($2P_r$) and coercive field (E_c) both increases gradually with the increase of (KCe) doping content. When the doping content is 0.3, the $2P_r$ and E_c for KCSNBT-*x* simultaneously exhibit maximum value of 16.4μC/cm^2 and 59kV/cm, respectively. The $2P_r$ is much higher than that of pure SNBT ceramic, indicating that the ferroelectric property of SNBT ceramic has been enhanced by (KCe)-doping. The remarkable enhancement in ferroelectric polarization could be mainly attributed to the crystal lattice distortion originated from the replacement of the *A*-site Sr^{2+} by K^+ and Ce^{3+}, which is also substantiated by XRD results that lattice parameters *a*, *b*, and *c* varied with increasing *x* values. Moreover, the ferroelectricity in BLSFs is related to the tilting of oxygen octahedral BO_6 from the *c* axis and the rotation in the *a*-*b* plane[30, 31]. In view of the difference of mean ionic radius caused by the introduction of (KCe) into the SNBT ceramics, the tilting and rotation of oxygen octahedral TiO_6 have been enlarged, which should be responsible for the enhanced ferroelectric property[32]. Meanwhile, the increased E_c is consistent with the assumption (**Fig.4**) that oxygen vacancies are formed. Under high electric fields, the mobile oxygen vacancies can assemble at the low energy domain walls, and thereby hinder domain switching due to domain pinning[33]. In order to further realize the polarization state of KCSNBT-*x* ceramics**,** the polarization current curves of the ceramics were collected, as shown in **Fig. 5(b).** One sharp polarization current peak could be observed when the applied electric field reached E_c, indicating the ferroelectric domain could be easier to switch when the driving electric field increase to E_c[34].

Fig.6 gives the thermal annealing behavior of piezoelectric constant (d_{33}) of the KCSNBT-*x* ceramics depolarized at different temperatures for holding 10 min. The excellent piezoelectric coefficient is founded to be 23 pC/N when *x* is 0.1 as shown in **Table 2**, which is higher than the reported results in other Aurivillius material systems

(**Table 1**)[22-24]. In addition, the values of d_{33} were not zero when the depolarization temperature was higher than the first dielectric anomalies (~400□). However, when the depolarization temperature was higher than the second dielectric anomalies, the d_{33} was zero. Therefore, in the x range of 0~0.3, the KCSNBT-x piezoelectric materials underwent a ferroelectric–ferroelectric transition at the first dielectric anomalies and a ferroelectric-paraelectric transition at the second dielectric anomalies temperatures, as shown in **Fig.3**. Moreover, the inset of **Fig.6** clearly shows that the piezoelectric constant (d_{33}) of KCSNBT-0.1 ceramic remains almost unchanged (22pC/N, only decrease by 4 %) at temperatures below 400℃, indicating that the ceramic has excellent temperature stability, so that it is very tolerant to thermal annealing and might be an appropriate candidate for high temperature applications.

4. Conclusion

KCSNBT-x ceramics were prepared by conventional solid state sintering method, and their structure and electrical properties were studied. The KCSNBT-x ceramics presented a typical layered perovskite structure. The morphologies of Aurivillius ceramics show the grains of all the samples are all well-defined and the plate-like morphologies of samples can be obtained. The T_c increases slightly from 562℃ to 567℃. The activation energy (E_a) values of the ionic conductivity suggested defects were related to oxygen vacancies. The $2P_r$ increase up to be 16.4μC·cm^{-2} with (KCe)-modifications. Meanwhile, the ceramics show excellent thermal stability when the annealing temperature below 400℃. As a result, a high T_c, d_{33} and good thermal stability have been attained in KCSNBT-x ceramics. Therefore, such a material system is a potential candidate for high-temperature piezoelectric applications.

Acknowledgement

This work was supported by the National Natural Science Foundation of China (No. 51372110, 51402144, 51302124, 51302025), National High Technology Research and Development Program of China (No. 2013AA030801), Science and Technology Planning Project of Guangdong Province, China (No. 2013B091000001), Independent innovation and achievement transformation in Shandong Province special, China (No. 2014CGZH0904), The Project of Shandong Province Higher Educational Science and Technology Program (No. J14LA11, No.J14LA10), Research Foundation of Liaocheng University (No. 318011301, No.318011306).

References

1. B. H.Park, B. S. Kang, S. D.Bu, T. W. Noh and J. Lee, *Nat*, 1999, **401**, 682-684.
2. P. Xiao, Y. Guo, M. Tian, Q. Zheng, N. Jiang, X. Wu, Z. Xia and D. Lin, *Dalton T*, 2015, **44**, 17366-17380.
3. J. S. Kim, M. S. Jang, I. W. Kim and K. S. Lee, *J electroceram*, 2006, **17**, 129-133.
4. J. Xiao, H. Zhang, Y. Xue, Z. Lu, X. Chen, P. Su, F. Yang and X. Zeng, *Ceram Int*, 2015, **41**, 1087-1092.
5. S. Ye, J. Fuh, L. Lu, Y.-l. Chang and J.-R. Yang, *RSC Adv*, 2013, **3**, 20693-20698.
6. J. Wu, Y. Wang and H. Wang, *RSC Adv*, 2014, **4**, 64835-64842.
7. A. Kaushal, S. M. Olhero, B. Singh, R. Zamiri, V. Saravanan and J. M. F. Ferreira, *RSC Adv*, 2014, **4**, 26993-27002.
8. Y. Zhong-Ran, C. Rui-Qing, X. Zhi-Jun, H. Ji-Gong and L. Guo-Rong, *J Inorg Mater*, 2015, **30**, 989-994.
9. L. Fei, Z. Zhou, S. Hui and X. Dong, *Ceram Int*, 2015, **41**, 9729-9733.
10. Q. Chen, Z. Xu, R. Chu, J. Hao, Y. Zhang, G. Li and Q. Yin, *Phys B*, 2010, **405**, 2781-2784.
11. J. D. Bobić, M. M. Vijatović Petrović, J. Banys and B. D. Stojanović, *Ceram Int*, 2013, **39**, 8049-8057.
12. D. Peng, H. Zou, C. Xu, X. Wang and X. Yao, *J Alloy Compd*, 2013, **552**, 463-468.
13. W. Ji, R. Chu, Z. Xu, J. Hao, R. Cheng, X. Chen and Y. Xu, *J Mater Sci: Mater Electron*, 2015, **26**, 5686-5689.
14. L. Sun, Q. Chen, D. Wu, J. Wu, Z. Tan, D. Xiao and J. Zhu, *J Alloy Compd*, 2015, **625**, 113-117.
15. L. Sun, Q. Chen, J. Wu, Z. Peng, Z. Tan, D. Xiao and J. Zhu, *Ceram Int*, 2014, **40**, 14159-14163.
16. Z. Yao, R. Chu, Z. Xu, J. Hao, D. Wei and G. Li, *J Mater Sci: Mater Electron*, 2015, **26**, 8740-8746.
17. L. Nibou, A. Aftati, M. El Farissi and J.-P. Mercurio, *J Eur Ceram Soc*, 1999, **19**, 1383-1386.
18. C.-H. Lu and C.-H. Wu, *J Eur Ceram Soc*, 2002, **22**, 707-714.
19. E. Khomyakova, J. Pavlic, M. Makarovic, H. Ursic, J. Walker, T. Rojac, B. Malic and A. Bencan, *J Eur Ceram Soc*, 2015, **35**, 4163-4171.
20. Z. Xu, R. Chu, J. Hao, Y. Zhang, Q. Chen, L. Zhao, G. Li and Q. Yin, *J Alloy Compd*, 2009, **487**, 585-590.
21. Z. Peng, Q. Chen, D. Liu, Y. Wang, D. Xiao and J. Zhu, *Curr Appl Phys*, 2013, **13**, 1183-1187.
22. P. Nayak, S. R. Mohapatra, P. Kumar and S. Panigrahi, *Ceram Int*, 2015, **41**, 9361-9372.

23. X. Meng, W. Ma, T. Chen, M. Wang and Y. Guo, *Electron Mater Lett*, 2015, **11**, 902-905.
24. R. Singh, V. Luthra, R. S. Rawat and R. P. Tandon, *Ceram Int*, 2015, **41**, 4468-4478.
25. C. Diao, H. Li, Z. Chen and H. Zheng, *Ceram Int*, 2016, **42**, 621-626.
26. V. Senthil, T. Badapanda, A. Chandrabose and S. Panigrahi, *Mater Lett*, 2015, **159**, 138-141.
27. A. Peláiz-Barranco and Y. González-Abreu, *Solid State Commun*, 2009, **149**, 2082-2084.
28. A. Palanduz and D. Smyth, *J electroceram*, 2003, **11**, 191-206.
29. S. Bharadwaja and S. Krupanidhi, *J Appl Phys*, 1999, **86**, 5862-5869.
30. J. Rödel, W. Jo, K. T. Seifert, E. M. Anton, T. Granzow and D. Damjanovic, *J Am Ceram Soc*, 2009, **92**, 1153-1177.
31. Z. Yao, H. Liu, Y. Liu, Z. Wu, M. Cao and H. Hao, *Appl Phys Lett*, 2008, **92**, 2905.
32. T.-L. Zhao, C.-M. Wang, C.-L. Wang, Y.-M. Wang and S. Dong, *Mater Sc Eng: B*, 2015, **201**, 51-56.
33. A. Khokhar, P. K. Goyal, O. P. Thakur, A. K. Shukla and K. Sreenivas, *Mater Chem Phys*, 2015, **152**, 13-25.
34. R. Cheng, C. Wang, Z. Xu, R. Chu, J. Hao, H. Li, W. Li, J. Du and G. Li, *RSC Adv.*, 2015, **5**, 90508-90514.

Figures captions

Fig.1. XRD patterns of KCSNBT-*x* ceramics sintered at 1180℃; Inset: Detailed information on the response of the variation of lattice parameters as a function of *x*

Fig.2. SEM micrographs of KCSNBT-*x* ceramics: (a) *x*=0, (b) *x*=0.1, (c) *x*=0.2, (d) *x*=0.3,

Fig.3. Temperature dependence of dielectric constant (ε) and loss (tanδ) of KCSNBT-*x* ceramics measured at 10 kHz. Inset: ln(1/ε-1/ε_m) as a function of ln(T-T_m) at frequency of 10 kHz of KCSNBT-*x* ceramics.

Fig.4. Temperature dependence of resistivity of KCSNBT-*x* ceramics

Fig.5. (a) *P*-*E* hysteresis loops of KCSNBT-*x* ceramics with different *x* at 180℃; (b) *I*-*E* loops of KCSNBT-*x* ceramics at 180℃.

Fig.6. Annealing temperature dependence of piezoelectric coefficient (d_{33}) for KCSNBT-*x* specimens, the inset shows the relative d_{33} (%) values of KCSNBT-0.1 sample.

Figure captions

Figure 1

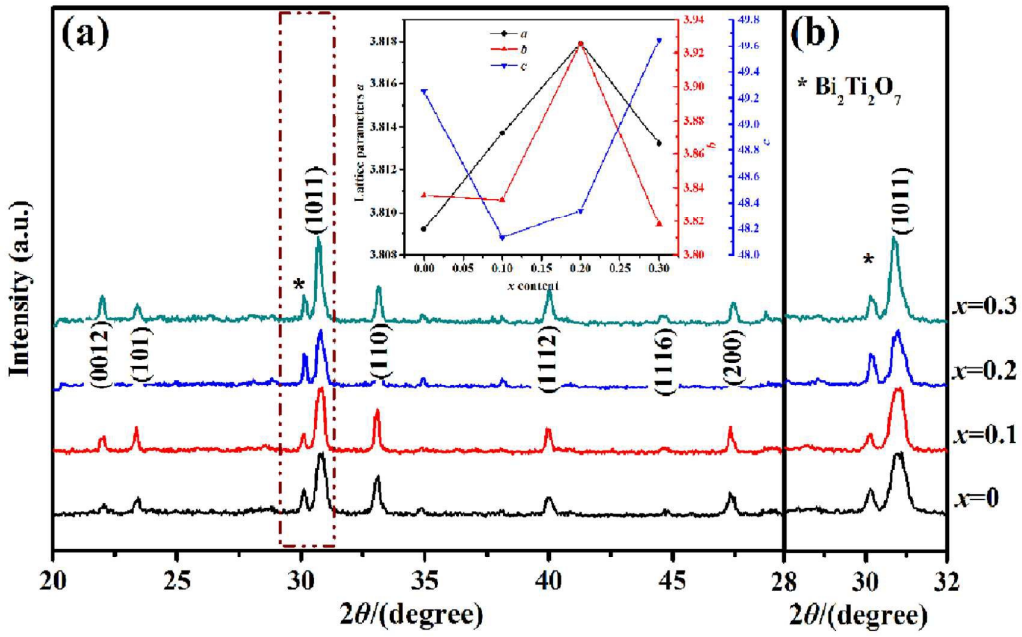

Figure 2

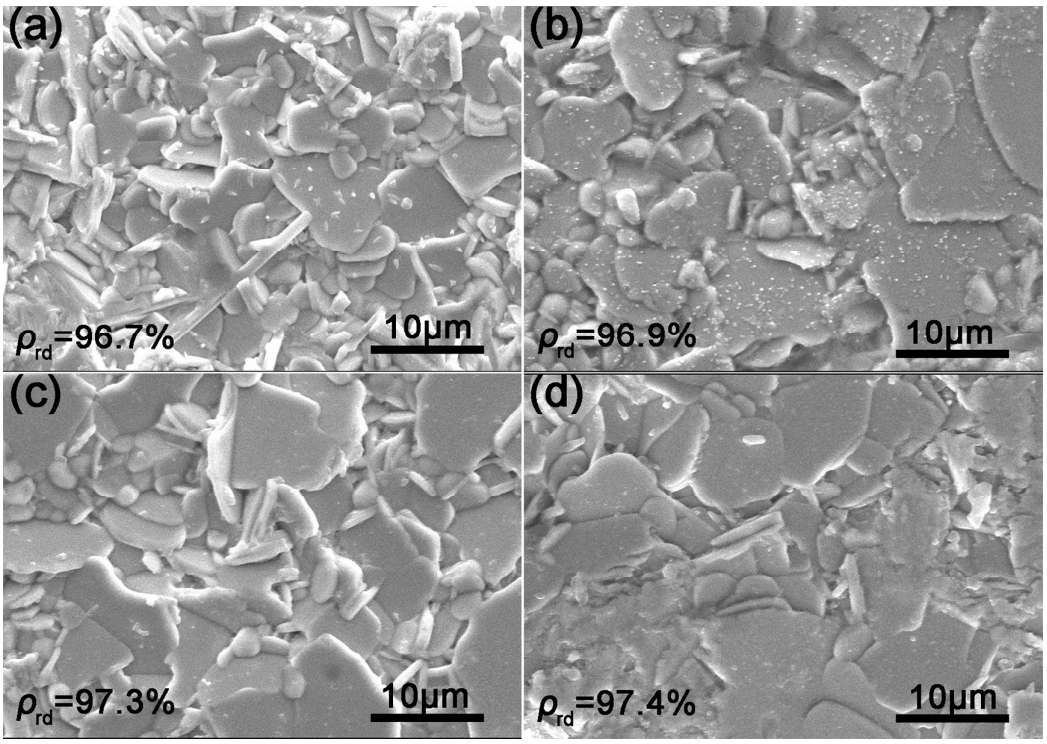

Figure 3

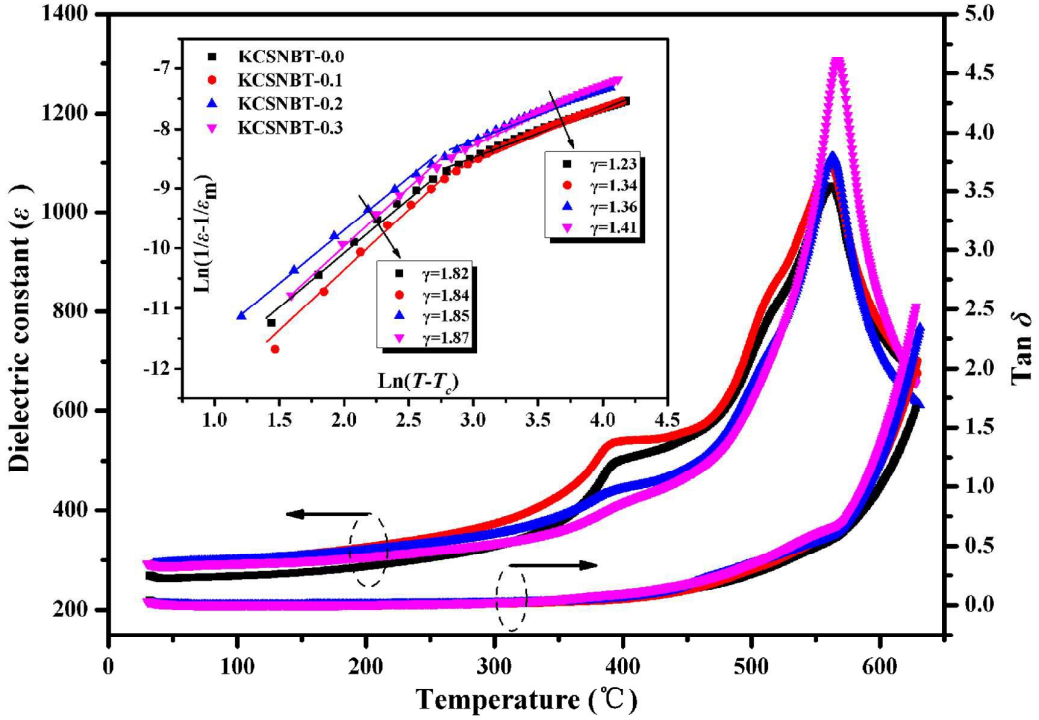

Figure 4

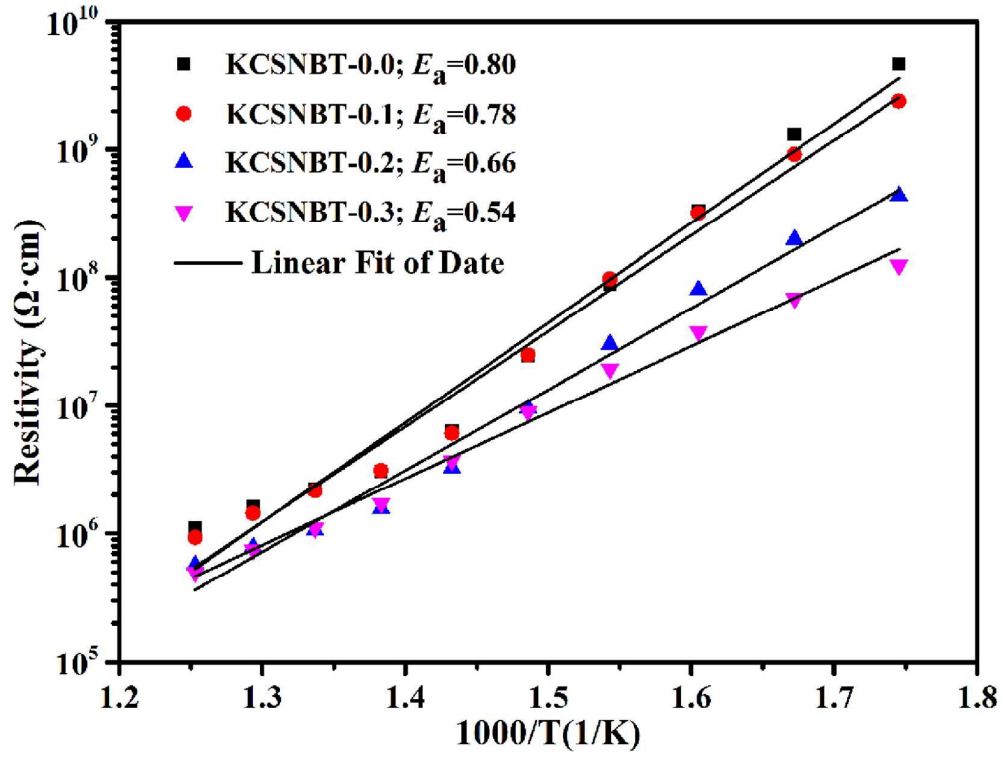

Figure 5

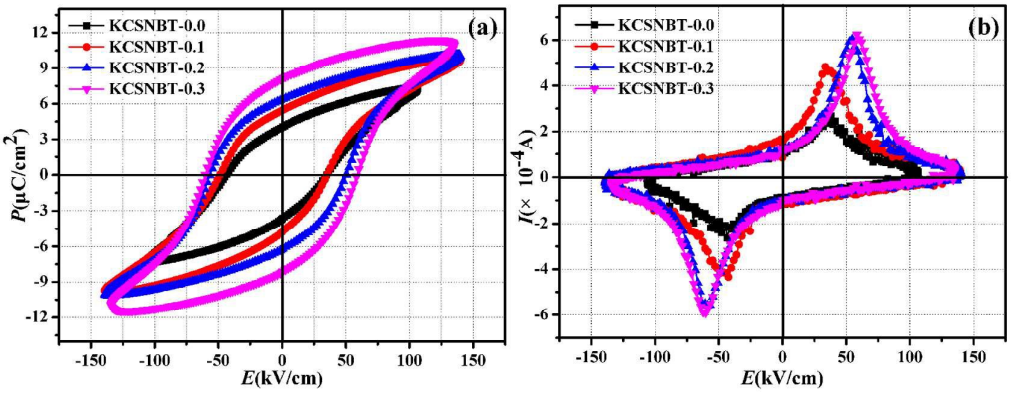

Figure 6